

# Using Entropy to Detect Quantum Phase Transitions

Presented to the S. Daniel Abraham Honors Program

in Partial Fulfillment of the

Requirements for Completion of the Program

Stern College for Women

Yeshiva University

April 29, 2013

David J. Kollmar

Mentor: Dr. Lea F. Santos, Physics

## I. Overview

In this thesis we discuss how entropy can be used to detect quantum phase transitions. We examine the invariant correlational entropy for two types of spin-1/2 systems: the Heisenberg nearest neighbor and next nearest neighbor model. We compare our results to results from other methods of detecting phase transitions such as the computation of the fidelity between two different low energy states close to the critical point. We find that the invariant correlational entropy can detect transitions, even those of infinite order which are generally hard to detect. However, it is not conclusive whether there are significant advantages of this method over others already in use. One possible advantage is that the invariant correlational entropy is basis independent, unlike the fidelity which is basis dependent.

The structure of this thesis is as follows: Section II provides introductions to concepts that are used later. We begin with a brief discussion about quantum mechanics, which is then followed by a discussion of what are quantum phase transitions and entropy, and why they are important. In Section III we explain electron spin and the Zeeman Effect. This is a preparation for the spin-1/2 models studied here. One of these models is discussed and analyzed in Section IV. The eigenvalues, eigenvectors, and symmetries of the system are studied, as well as their relationship with the system dynamics. In Section V we introduce a second spin-1/2 model and use both spin models to present our studies of the detection of quantum phase transitions. Our concluding remarks appear in Section VI.

## II.1. Introduction to Quantum Mechanics

Much of what we see in the world around us can be described by classical physics. In the realm of extremely small objects, however, these laws break down. Instead, the laws which apply are the ones of quantum mechanics.

One of the main goals of quantum mechanics is to predict the probability of a particle being in a specific place at a specific time. To do this, it is necessary to solve the Schrodinger Equation:

$$i\hbar\frac{\partial\Psi}{\partial t} = H\Psi, \quad (1)$$

where  $\Psi$  represents the wave function of the particle and  $H$  represents the Hamiltonian. The wave function is significant because  $|\Psi(x,t)|^2$  gives the probability of the particle being at position  $x$  at time  $t$ . When the particle is observed, the wave function collapses, and the particle is measured as being in only one place.

However, the wave function only gives a probability for a location at a given time; it is impossible to know both a particle's location and its momentum. This is a result of the Heisenberg Uncertainty Principle,

$$\sigma_x\sigma_p \geq \frac{\hbar}{2}. \quad (2)$$

This equation states that the uncertainty in the precision of the measurements for the position and the momentum must exceed a certain value.

In order to solve Schrodinger's equation to find the wave function, we must first identify the expression for the Hamiltonian. This operator describes the energy of the system. Depending on the Hamiltonian, it may be possible to solve the differential equation and find  $\Psi(x,t)$  [1]. When an analytical solution is not viable, we can still resort to numerical approximations, which is the approach we take in this thesis.

## II.2. Introduction to Quantum Phase Transitions

In classical physics, a thermal phase transition occurs when the temperature of a material reaches a critical point and the material undergoes a change in state. As an example, take water/ice. When water is in the liquid phase, the molecules can move around freely, although there are still intermolecular forces between them. Because of the free movement, there is a high level of entropy, often defined as disorder, within the system. As the water is cooled, however, the molecules slow down and their kinetic energy is therefore lowered. The molecules begin to arrange themselves into a lattice structure, resulting in lower entropy, and the transition from water to ice eventually occurs. A similar process takes place with thermal phase transitions of other materials. In thermodynamics, phase transitions are understood as a desire of the system to minimize its free energy  $F=E-TS$ , where  $E$  is energy,  $T$  is temperature, and  $S$  is entropy. As the temperature goes down, the entropy decreases. The only way to guarantee that  $F$  will be minimized is if the energy also decreases, as in the crystal structure. Similarly, as heat is added to the system and its energy increases, the entropy also increases, keeping  $F$  small. Thermal phase changes are common phenomena and are easy to detect because they usually involve visible changes, such as the transition from water to ice.

At absolute zero temperature ( $T = 0$  Kelvin), according to classical physics, we would expect the molecules to stop moving and the phase to be stable. However, at low temperatures, the classical laws break down and quantum physics takes over [1]. In the quantum domain, the so-called uncertainty principle states that it is not possible to simultaneously specify both the position (potential energy) and the momentum (kinetic energy) of each molecule. The delicate balance between the two energies, similar to the

balance between energy and entropy in the case of thermal phase transitions described above, implies the existence of quantum fluctuations, leading to more than one possible phase even at  $T = 0$  K [2].

There are several types of quantum phase transitions, and the phases involved have different macroscopic properties which can be experimentally detected [2,3]. One type relates to the magnetic properties of the system. Spin is an intrinsic property of elementary particles associated with their angular momentum, as will be explained later in this thesis. Electrons, protons, and neutrons, the constituents of matter, have spin-1/2, which implies that in a strong magnetic field, they can align either parallel or antiparallel to this field. In a spin-1/2 system, when all spins are pointing in the same direction, the material is said to be ferromagnetic. When the spins point in random directions, the material is said to be paramagnetic. At 0 K, a quantum phase transition can occur when a material switches from being paramagnetic to being ferromagnetic.

Another type of quantum phase transition is the switch from a superfluid to an insulator. At very low temperatures, a bosonic system becomes a superfluid, a state in which the particles flow past each other with no viscosity. However, it is possible to use optical lattices to organize the supercool atoms into a crystal. Optical lattices are formed by standing waves made of lasers [4]. As the periodic potential of these waves increase, the bosons become locked into the areas with the lowest potential. Eventually, the bosons become an insulator because they are no longer free to flow.

A property common to both of these types of transitions, as well as others, is that the Hamiltonians of the system have two competing terms. These terms are related to each other by a parameter. When the parameter has one value, one term dominates the system, and the

system is in one phase. At other values for the parameter, however, the other term can dominate the system, and the system will be in another phase [5].

Quantum phase transitions occur in systems of interacting particles, because of discontinuities in their thermodynamic functions, or the opening or closing of an energy gap. There are several orders of transitions. First order transitions occur when there is a discontinuity in the energy density of the system. These types of transitions are easiest to detect. Second order transitions occur when the energy density of the system is continuous, but its first derivative has a discontinuity [6]. Another category of transitions are Berezinskii-Kosterlitz-Thouless transitions, or BKT transitions. These transitions are referred to as infinite order because they are always continuous, so they are the hardest to detect [7]. When there are interactions between particles, especially if they are strong, the properties of the whole system (including energy) cannot be obtained from the sum of its constituents. Therefore, instead of studying real systems, models of simpler systems, such as certain spin systems, must be used [8]. These systems are good choices because they are typical many body systems, and are good models of some real materials such as cupric oxides [9]. The ground state and first excited state of these systems are examined to detect transitions.

Through numerical studies, we have been studying spin systems for which the parameters leading to quantum phase transitions are already known. This allows us to analyze whether the invariant correlational entropy can also detect the transitions in spin systems.

### **II.3. Introduction to Entropy**

The term entropy has many definitions [10]. One of the most commonly used definitions is the amount of disorder within a system. Another definition, based on studies in probability, is the amount of information that must be learned in order to determine the value of something in the system. Some scientists such as Arie Ben Naim argue that this definition is the better one [11]. The definition of entropy that we are particularly interested in is called invariant correlational entropy, which has already been used to detect quantum phase transitions in nuclear systems. This type of entropy measures how responsive a system is when one of its parameters is changed [12].

The purpose of this project is to learn more about quantum phase transitions such as those mentioned earlier and find out if they can be detected by observing the system's invariant correlational entropy. A peak in this quantity indicates a critical region.

### **II.4. Why are Entropy and Quantum Phase Transitions Important to Study?**

The study of entropy and quantum phase transitions is important for several reasons. First, it will shed light on concepts which are fundamental to physics but which little is already known. Entropy is important because it is used to explain the notion of irreversibility in nature, the idea that there is a preferential direction in time, the so-called "time's arrow," From the second law of thermodynamics, systems prefer to go from states of less entropy to states of more entropy.

Finding evidence of phase transitions is also important. Different phases have different properties. An example of this can be seen regarding the thermal phase transition mentioned above. Sound propagates differently in a liquid and in a solid, and the two phases

conduct heat and electricity differently. Quantum systems, such as the spin systems we have been studying, also have different properties in different phases. For example, they can exhibit transitions from a paramagnetic to a ferromagnetic phase. The latter responds much stronger to an applied magnetic field and has important applications in modern technology. Ferromagnetism is the basis for many electrical and electromechanical devices such as electromagnets, electric motors, generators, transformers, and magnetic storage such as tape recorders, and hard disks. Delineating different phases is therefore essential for differentiating domains where different properties will come into play. Additionally, phase changes surround us daily on the macroscopic level, and it is important to understand how these macroscopic changes are caused by microscopic fluctuations. However, identifying and characterizing quantum phase transitions are far from trivial. The purpose of this research is to help provide a new method to detect quantum phase transitions and so contribute to the various recent theoretical and experimental works in this direction.

Another reason why this research is important is because there have been many recent experiments in the field, such as those with optical lattices mentioned earlier [13]. These experiments are being conducted to study quantum phase transitions, but theory is needed to explain the experimental results. This project will focus more on the theory and the computational aspect of the ongoing research.

### **III.1. Introduction to Electron Spin and Spin-1/2**

Atoms are made up of a nucleus, which contains protons and neutrons, and electrons, which orbit the nucleus. Based on the quantum mechanical view of the electron, the electron travels as a wave, although it is detected as a particle [14]. However, the electron is confined

to certain quantized, or discrete, energies; the electron cannot go from one energy level to another without gaining or emitting energy. From the Schrodinger equation we can find the probability that an electron will be found in a given area, although we cannot know an electron's position and momentum simultaneously with infinite precision because of the Heisenberg uncertainty principle. The region where the electron is most likely to be found is called its orbital.

The orbital of the electron can be described by its quantum numbers, integer numbers which are results of the Schrodinger equation. The first three quantum numbers define the electron's location in space. The first quantum number is  $n$ , the principal quantum number. This number, which can be any positive integer, defines the energy of the electron and its resultant distance from the nucleus. An electron with more energy will be further away. The next quantum number is  $l$ , the angular momentum quantum number. Because the electron orbits the nucleus, it will have orbital angular momentum. This angular momentum can have any integer value from  $l=0$  to  $l=n-1$ . The angular momentum gives the shape of the electron orbit, such as a sphere, dumbbell, or four-leaf clover. The third quantum number is  $m_l$ , or the magnetic quantum number. The electron is a moving negatively charged particle, and a moving charge creates a magnetic field. When the charge is moving in a circle, the field approximates that of a magnetic dipole, with a dipole moment in the same direction as the angular momentum. The magnetic quantum number can vary from  $-l$  to  $+l$ , and determines the orientation of the electron's orbit. For example, picture a dumbbell. There are several choices for how to orient it along one of the Cartesian axes: along the x, y, or z axis. This choice will determine the system's magnetic dipole number [15].

The Stern-Gerlach experiment was created in order to test the quantum theory for electrons. As we have already shown, the electron's orbit around the nucleus creates a magnetic dipole moment. When an atom has more than one electron, often the electrons are paired and their effects cancel. However, for some types of atoms, there are unpaired electrons, each with its own magnetic dipole moment, and their effects combine to give the whole atom a magnetic dipole moment. One such atom is silver. In the Stern-Gerlach experiment, silver atoms were shot through a magnet at a detector. Based on its magnetic dipole moment, the atom would be deflected towards the north or south part of the magnet before hitting the detector.

Classically, it would be expected that the location where the atoms would hit the detector would be distributed uniformly within a range of values, with the minimum and maximum determined by the magnetic dipole moment of the atom. This is because the magnetic dipole moment could be oriented in any direction in space, while only the z-component would be relevant to deflect it. Therefore, the z-components could be distributed uniformly, with a maximum when the magnetic dipole moment would be oriented up and with a minimum when the magnetic dipole moment would be oriented down. On the other hand, based on the quantum mechanical model of the atom, it would be expected that there would be several discrete bands of energies. This is because in the quantized view, there are discrete allowed values for the magnetic dipole moment and its orientation, and intermediate values are not allowed. Additionally, it would be expected that there would be an odd number of bands, with the middle band corresponding to no deflection. This is because the magnetic quantum number can vary from  $-l$  to  $+l$ , so it will give an odd number of values centered at zero.

When the experiment was performed, the results were two discrete bands, one above the area corresponding to no deflection and one below that area. Qualitatively, the results made sense, since they disproved the classical model of the electron and upheld the quantum mechanical model. However, quantitatively, the results were strange, because they did not match the expected odd number of bands centered at the midpoint. In order to figure out why the results came out the way they did, the experiment was repeated by Phillips, but this time using hydrogen atoms. These atoms have only one electron, so all effects are a result of the properties of the electron itself and not because of the interactions between electrons which can possibly be found in larger atoms. The new experiment, however, had the same results as the previous one.

Eventually researchers concluded that the reason for the unexpected result was a previously unconsidered quantity called spin. To explain spin, it is helpful to use the analogy of Earth orbiting the sun. Earth orbits the sun in an orbit which has the period of a year. This orbit gives the Earth orbital angular momentum. At the same time, Earth rotates along its own axis, rotating once a day. This rotation is called spin, and gives Earth a spin angular momentum. The electron is predicted to work in a similar way. The electron has spin, which gives it a spin angular momentum. This angular momentum also creates a magnetic dipole moment, which is stronger than the orbital magnetic dipole moment and accounts for the results of the experiment.

However, the analogy to Earth does not work completely. The Earth's spin around its axis can be broken down into individual clumps of dirt which orbit the axis—that is, the spin of the larger body is created by the orbits of its smaller components. However, this model does not work for electrons. First, electrons are a type of elementary particle, and elementary

particles are indivisible, so there is nothing analogous to the clumps of dirt. Also, if the electron were actually spinning, the velocity of the outer part of the electron could be calculated based on the experimentally-determined magnetic dipole moment of the electron. When such calculations were performed, the velocity exceeded that of light, which is not allowed based on Einstein's first law of relativity. Therefore, we say that electrons have an intrinsic quantity called spin, but that this does not correspond to any actual spinning motion.

Electron spin is associated with the fourth quantum number,  $m_s$ , or the electron spin magnetic quantum number. Since there were two bands in the Stern-Gerlach experiment, there are two possible values for  $m_s$ . One of these values is negative and one is positive, since one band was deflected up and the other was deflected down. Like the other quantum numbers, the difference between consecutive values is one. Therefore, we say that  $m_s$  can be  $+1/2$  or  $-1/2$ , and so we say that electrons have spin- $1/2$ . This is the only quantum number which has non-integer values. We can also say that a spin of  $+1/2$  corresponds to a spin up with respect to the direction of an external field, while a spin of  $-1/2$  corresponds to a spin down. There are other particles which have spins different from spin- $1/2$ , such as photons which have spin-1 [14,16,17].

### **III.2. Zeeman Effect**

Now that we understand spins, it is possible to understand the "Anomalous" Zeeman Effect. It had been known for some time that atoms emit different colors of light when an electron goes from a higher energy shell to a lower energy shell. Pieter Zeeman observed that when a magnetic field would be turned on, each band on the light spectrum would split into multiple bands. He explained that this was a result of the magnetic dipole moments that came

from the orbital angular momentum. This is because there will be slight energy differences as the orientation of the dipole with the magnetic field changes. However, there were some cases where there were extra lines, or they were further apart than expected. This was called the “Anomalous” Zeeman Effect. Researchers explained this as a result of the magnetization arising from the spin. When the spin is oriented parallel to the field, it has one energy value, and when it is antiparallel to the field, it has a different energy. The bands split because the spin can change when going from one shell to the other [17].

#### **IV.1. Spin-1/2 Chains**

Very often, we are dealing with not just one particle, but many interacting particles, in what is called a quantum many-body problem. Here, we deal with a one-dimensional spin-1/2 lattice, which is a spin-1/2 chain. In general, if there are “L” sites on the chain, there are  $2^L$  possible configurations of spins, because each spin-1/2 is a two-level system. Sometimes, we have more information, and so we can limit the number of configurations we consider. For example, in some systems, in addition to knowing the number of sites in the chain, we know that it conserves the total spin in the z-direction. This means that the Hilbert space is divided in subspaces, each with a fixed number (N) of spins pointing up. We would like to determine how many possible configurations of spins there are in each subspace. To figure this out, we use probability. If we had L different types of spins, we would have L! different configurations. However, it is impossible for us to distinguish between two different up spins or between two different downspins. Therefore, we divide L! by N! and by (L-N)! to remove these redundancies. The possible number of configurations is then  $L!/(N!(L-N)!)$ .

Now that we know the number of possible configurations of spins, we would like to determine why some configurations are preferable to others. For example, there are some systems where all parallel spins is preferred, which are called ferromagnetic systems, while there are other systems where alternating spins is preferred, which are called antiferromagnetic systems. To explain this, it is important to know that systems try to minimize their energy when possible; the minimal energy is called the ground state, and higher energies are called excited states. We will see that depending on the parameters in the Hamiltonian, some systems will minimize their energy when they are ferromagnetic and others will reach the ground state when they are antiferromagnetic. The Hamiltonian can be written as a matrix, as will be explained below. Before explaining the Hamiltonian, though, we must explain the site basis, which is the basis we will use to write it.

## **IV.2. Introduction to the Site Basis**

In order to create the Hamiltonian matrix, we first need to choose a basis to represent it in. One appropriate basis is the site basis. In this basis, we represent up spins by ones and down spins by zeros. So, for example, a chain with four sites, the first two with up spins and the second two with downspins, would be written as  $|1100\rangle$ .

This representation of the site basis is physical and indicates the orientation of the spin in each site. It is useful when we want to compare adjacent spins. A more abstract representation corresponds to unitary vectors with the same dimension of the subspace. For example:

$$|1100\rangle = \begin{pmatrix} 1 \\ 0 \\ 0 \\ 0 \\ 0 \\ 0 \end{pmatrix} \quad \text{and} \quad |1010\rangle = \begin{pmatrix} 0 \\ 1 \\ 0 \\ 0 \\ 0 \\ 0 \end{pmatrix}. \quad (3)$$

### IV.3. Hamiltonian with Nearest Neighbor Couplings

Now that we have explained the site basis, we are ready to explain in depth the Hamiltonian of one of our systems, described by the Heisenberg model [18]:

$$H = \sum_{j=1}^L E_j S_j^z + \sum_{j=1}^{L-1} J (\Delta S_j^z S_{j+1}^z + S_j^x S_{j+1}^x + S_j^y S_{j+1}^y). \quad (4)$$

In the equation above, the  $S$ 's represent the spin operators. These operators are equal to half the Pauli operators

$$\hat{\sigma}^x = \begin{pmatrix} 0 & 1 \\ 1 & 0 \end{pmatrix}, \hat{\sigma}^y = \begin{pmatrix} 0 & -i \\ i & 0 \end{pmatrix}, \hat{\sigma}^z = \begin{pmatrix} 1 & 0 \\ 0 & -1 \end{pmatrix}, \quad (5)$$

since in our system we are allowing  $\hbar$  to equal 1.  $S_j^{x,y,z}$  will act only on site  $j$ . There are only nearest neighbor coupling between sites  $j$  and sites  $j+1$ .  $J$  and  $\Delta$ , the anisotropy parameter, determine the strengths of the coupling terms. In our system, we are allowing  $J$  to equal 1, to set the energy scale.

There are three main terms in the Hamiltonian above, which we will now analyze individually.

The first term is the one-body term. The expression is as follows:

$$\sum_{j=1}^L E_j S_j^z \quad (6)$$

This term is also referred to as the Zeeman splitting term, since it is related to the Zeeman Effect mentioned earlier. A spin up has energy  $E/2$ , and a spin down has energy  $-E/2$ . As a result, an up spin has more energy than a downspin, so we call an up spin an excitation. The

$E_j$ 's for each site can have a different value. When the  $E$ 's are all the same, the system is called a clean system. It only adds a constant to the diagonal of the Hamiltonian matrix and can therefore be ignored. If one of the  $E$ 's is different from the others, it is said that that site has a defect. For this thesis, we always used  $E$ 's equal so the one-body term never had an effect on the behavior of our system.

The second term is called the Ising interaction. The expression is as follows:

$$\sum_{j=1}^{L-1} J\Delta S_j^z S_{j+1}^z. \quad (7)$$

This term is a result of the interaction between neighboring sites. This term has the following effect on spins:

$$\begin{aligned} J\Delta S_j^z S_{j+1}^z |1_j 1_{j+1}\rangle &= +\frac{J\Delta}{4} |1_j 1_{j+1}\rangle \\ J\Delta S_j^z S_{j+1}^z |1_j 0_{j+1}\rangle &= -\frac{J\Delta}{4} |1_j 0_{j+1}\rangle \end{aligned} \quad (8)$$

In other words, if the two sites have spins which are parallel to each other, the term  $J\Delta/4$  is added, while if they are antiparallel, the term is subtracted. The values of  $\Delta$  can be used to explain the magnetic properties of some materials. The Ising interaction corresponds to the potential energy of the system [18]. For positive  $\Delta$ , parallel spins have more energy than antiparallel spins. Therefore, when  $\Delta$  is positive, the lowest energy the system can have is when all of the spins are anti-parallel to each other, such as  $|010101\rangle$ , because the value  $J\Delta/4$  is subtracted the maximum number of times. The material is therefore anti-ferromagnetic. When  $\Delta$  is negative, the ground state of the chain is when all of the spins are parallel, such as  $|111111\rangle$ . This is because the value  $-|J\Delta|/4$  is added the maximum number of times. The material is therefore ferromagnetic. In this thesis, we chose to select a positive value for  $\Delta$  and consider only the antiferromagnetic model.

Because of our basis, when we make the Hamiltonian matrix, the one-body term and the Ising interaction will be found only on the diagonal, and the flip flop term will constitute the off-diagonal elements [18].

The third term is called the flip flop term. The anisotropy parameter  $\Delta$  determines the relative strength of the Ising interaction and this term. The expression is as follows:

$$\sum_{j=1}^{L-1} J(S_j^x S_{j+1}^x + S_j^y S_{j+1}^y). \quad (9)$$

This term has the following effect on spins:

$$J(S_j^x S_{j+1}^x + S_j^y S_{j+1}^y) \left| 1_j 0_{j+1} \right\rangle = \frac{J}{2} \left| 0_j 1_{j+1} \right\rangle. \quad (10)$$

When either of the first two terms of the Hamiltonian is applied to the system, there is no effect on the direction of the spins in the system. However, the flip flop term causes antiparallel spins to swap the direction of their spin, and it therefore corresponds to the kinetic energy of the system [18]. To add this term to the matrix, we compare two basis vectors to see if the pair corresponds to a state before and after the spins have been flipped. First we compare corresponding sites of two basis vectors, keeping track of the number of differences and their locations. For the flip flop term, there must only be two differences, since there would be only two sites with their spins flipped. If those sites are one apart, this corresponds to adjacent antiparallel spins being flipped and there is therefore a flip flop term of  $J/2$  added. If the sites are further apart, there is no contribution to the flip flop term. Since the Hamiltonian matrix is a Hermitian matrix, therefore symmetric, we need to find only the off-diagonal elements above (or below) the diagonal elements.

The Hamiltonian as written in Equation (4) gives an open system, where the two ends of the chain do not couple with each other. This is indicated by the sums defining the coupling terms, which go from site 1 to site  $L-1$ . Each end site only communicates with the

one site adjacent to it, unlike the sites in the middle of the chain which can communicate with sites on both sides. The fact that sites at the edges only couple with one other site leads to “Border Effects.” If the summation had been to  $L$  instead of to  $L-1$ , it would have indicated a closed system, where the two ends of the chain communicate with each other. In this latter case each member of the chain couples with two other members, and there is no border effect. It is as if instead of having the sites in a line, we have them in a ring. The system is translational invariant; if we translate the sites of the ring, it will have the same energy. For example, in a closed system  $|1000\rangle$  has the same energy as  $|0100\rangle$ , which is not the case with an open system.

The Hamiltonian operator commutes with the total spin in the  $z$  direction. Therefore, there will be several independent subspaces, each corresponding to a different total spin in the  $z$ -direction. When writing the code, we consider each block separately. While the dimension of the larger Hamiltonian is  $2^L$ , the dimension of each block is  $L!/(N!(L-N)!)$  (see the section titled “**Spin Chains**” above).

We can find the eigenvalues and eigenstates of the Hamiltonian matrix “ $H$ ” by diagonalizing it. To find the eigenvalues analytically, subtract a variable  $\lambda$  from each of the diagonal elements of  $H$ . Find the determinant of the new matrix, which will be a polynomial with the degree of the dimension of the matrix. Find the solution of the equation if the polynomial is set to zero; the solutions are the eigenvalues. The eigenvectors are then the non-zero vectors that give zero when multiplied by  $H-\lambda I$  (where  $I$  is the Identity Matrix). This method works because the determinant of  $H-\lambda I$  must be zero so that the eigenvectors can be non-zero.

The eigenvalues of the Hamiltonian matrix represent the energies in the system. The eigenstates are linear combinations of basis states.

#### IV.4. Spectrum

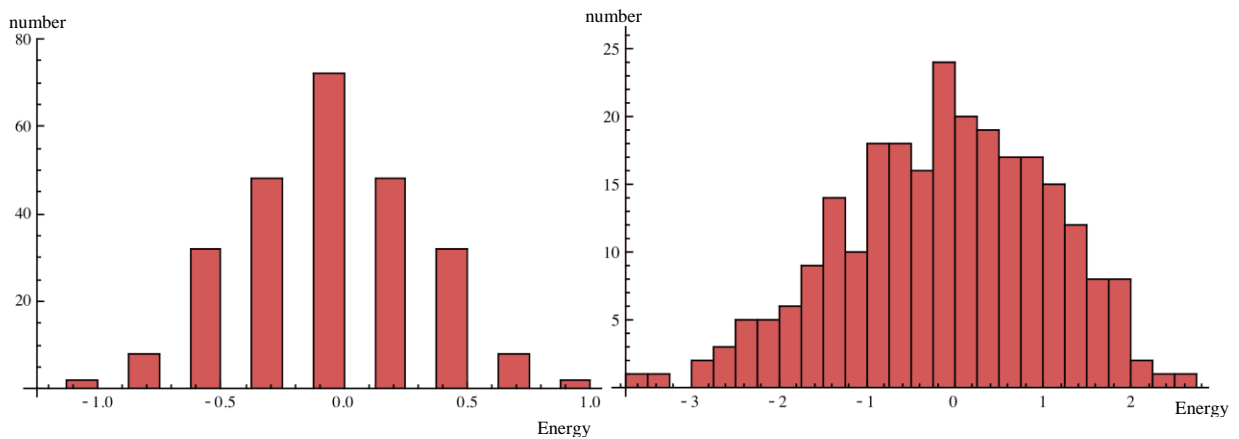
First, we will study the static properties of the system. We will start by discussing the case when there is no flip flop term, and will then extend this case for when the flip flop term is included to study the spectrum of the whole Hamiltonian.

When the system is clean and there is no flip flop term, the Hamiltonian matrix will be a diagonal matrix with all elements a multiple of  $J\Delta/4$ .

Some interesting observations can be made about the different values for the diagonals. There is a set step between each value of the diagonal, which is different for when the chain is open or closed. When the chain is open, there is a step of  $J\Delta/2$  between each value. This is because there is a maximum of  $L-1$  parallel couplings. When we break a string of ones or zeros, we lose energy, since (for positive  $\Delta$ ) parallel spins have higher energy than antiparallel spins. In this case, when one parallel coupling becomes antiparallel, the value of  $J\Delta/4$  is added one less time and subtracted one more time, making a net difference of  $J\Delta/2$ . The energy of the basis vectors is given by  $[2p-(L-1)]*J\Delta/4$ , where  $p$  is the number of pairs of parallel spins. On the other hand, the difference between values on a closed chain will be  $J\Delta$ . This is because there is a maximum of  $L$  parallel couplings. Since the chain is closed, there must always be an even number of antiparallel couplings; because there is no border to absorb one of the couplings, each set of zeros must have ones on both sides. Therefore, when two parallel couplings become antiparallel, the value of  $J\Delta/4$  is added two less times and

subtracted two more times, making a net total of  $J\Delta$ . The energy of the basis vectors is given by  $(2p-L)*J\Delta/4$ .

Another observation is that while the energy values themselves are dependent on  $J\Delta$ , because they are a multiple of  $J\Delta/4$ , the number of different values is a function of only  $L$  and  $N$ . We can see their distribution by making a histogram (see Fig. 1). This type of graph analyzes data by counting how many values there are in different intervals, which are called bins. It plots the number of values vs. the value of the interval. In the special case of an open chain when  $L$  is even and  $N$  is  $L/2$ , the histogram is symmetric. There are  $L-1$  bars. Depending on the size of the chain, we find one (as in the left panels of Fig. 1) or three (not shown here) bars of maximum height in the middle. The successive bars on each side decrease until the end bars, which each have just two states. Each isolated band of the graph corresponds to an energy band. Each basis vector has a different energy and therefore belongs to a different band. If the bins are made a good size such as  $J\Delta/4$ , the gaps between the different bands are clearly seen (see Fig. 1, both left panels).



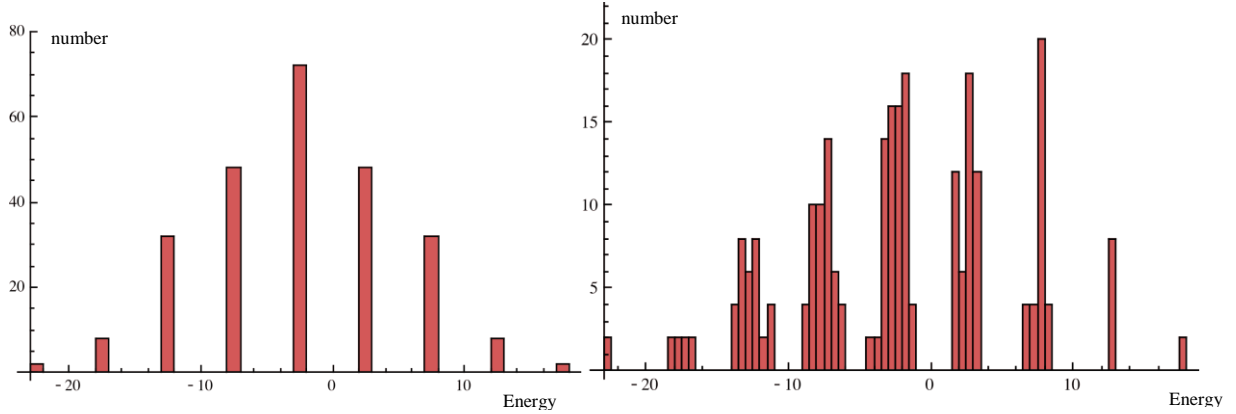


**Figure 1:** Spectrum of the spin  $\frac{1}{2}$  system with nearest neighbor couplings and open boundary conditions;  $L=10$ ,  $N=5$ . Top panels:  $\Delta=0.5$ . Bottom panels:  $\Delta=10$ . Left panels: only diagonal elements. Right panels: complete Hamiltonian with Ising and flip flop terms.

We are now ready to add in the flip flop term. Now, our matrix has values in the off-diagonal elements. Therefore, instead of analyzing only the diagonal, we will analyze the eigenvalues of the matrix (for a diagonal matrix, the eigenvalues are the same as the values on the diagonal). It is now the eigenvalues, not the diagonal elements, which correspond to the different energies on the spectrum. When we make the histogram, we see that depending on the value of  $\Delta$  the gap between the energy bands may disappear. For example, when  $\Delta$  is small, such as in the top right panel of Fig. 1, the energy bands run in to each other instead of remaining separate. However, when  $\Delta$  is high, such as in the bottom right panel of Fig. 1, the graph is similar to the graph from when there was no flip flop term. The flip flop term has a negligible role with respect to the dominant Ising interaction, and is not strong enough to couple basis vectors from different bands.

#### IV.5. Inverse Participation Ratio

The band structure is reflected into the level of delocalization of the eigenstates with respect to the site-basis. The level of delocalization can be measured with the inverse

participation ratio, or IPR, which is also known as the number of principal components, or NPC:

$$IPR^{(j)} \equiv \frac{1}{\sum_{k=1}^D |a_k^{(j)}|^4}. \quad (11)$$

In this equation, the absolute values are raised to the fourth power instead of squared because our vectors are normalized, so the sum of the squares of their elements will always be one.

If the result of the IPR is high, this means that the eigenstate is highly spread among the basis vectors, or delocalized. If the result is low, it means that the eigenstate is localized. We find the IPR for each eigenvector within a system, and we also find the average IPR for different systems with different  $J\Delta$ 's. A graph of the IPR for each eigenvector vs. the energy corresponding to that eigenvector will approximate the Gaussian shape, more so as  $\Delta$  increases (see Fig. 2). This form reflects the density of states, which is also Gaussian.

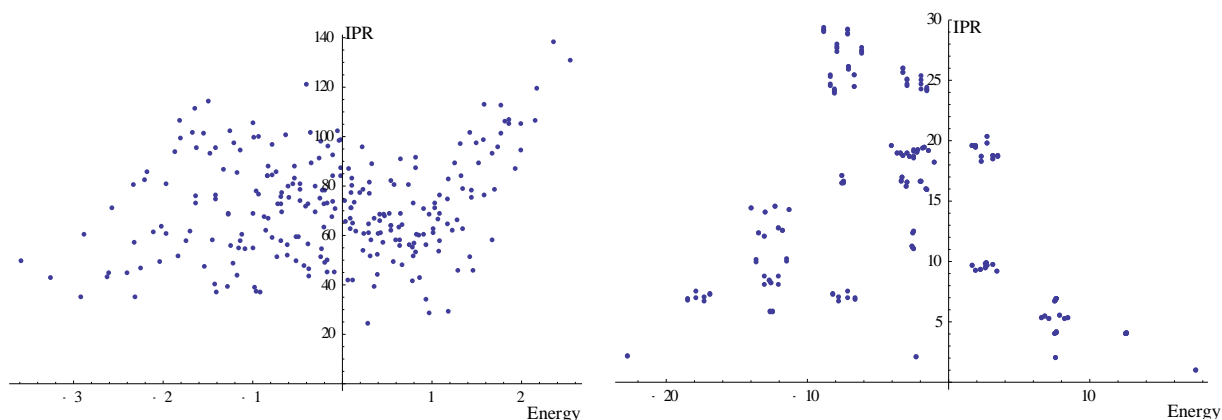


**Figure 2:** IPR vs. energy for the spin  $\frac{1}{2}$  system with nearest neighbor couplings and open boundary conditions;  $L=10$ ,  $N=5$ . Left panel:  $\Delta=0.5$ . Right Panel:  $\Delta=10$ .

When graphing the IPR averaged over all of the eigenvectors in a system vs.  $\Delta$ , we find that as  $\Delta$  increases, the IPR decreases at a fast rate, as seen in Fig. 3. This makes sense because when  $\Delta$  is low, the Ising interaction is overpowered by the flip flop term, which allows more basis vectors to contribute significantly to the eigenstates. Therefore, the system

will be more spread out among the basis vectors. When  $\Delta$  is high, though, the Ising interaction will overcome the flip flop term. The flip flop term is not strong enough to couple basis vectors from different energy bands, and the eigenstates will be restrained to configurations with the same energy. Therefore, the system will be localized onto only a few states.

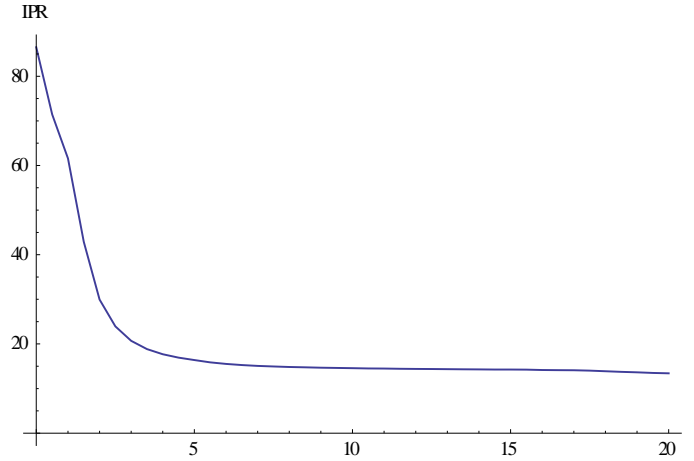


**Figure 3:** Average IPR vs.  $\Delta$  for the spin  $\frac{1}{2}$  system with nearest neighbor couplings and open boundary conditions;  $L=10$ ,  $N=5$ .

#### IV.6. Dynamics

If we start with a given initial state which is not an eigenstate of the system, we are able to find how the state changes over time. To do this, we must solve Schrodinger's equation for  $\Psi(x,t)$ . If the Hamiltonian does not depend on time, we can look for solutions of the kind  $\Psi(x,t) = \psi(x)\phi(t)$ . It is then possible to separate the equation into two parts, one of which is time dependent and the other of which is time independent. Since the two sides must be equal, they can then each be set equal to a constant  $E$ , which leaves two ordinary differential equations to solve:

$$H\psi = E\psi \quad (12)$$

$$\frac{\partial \Phi}{\partial t} = -\frac{iE}{\hbar} \Phi \quad (13)$$

When examining  $\Psi(x,t)$ , we find that  $\psi(x)$  represents the eigenstates of the Hamiltonian and  $E$  represents its eigenvalues. The values of  $\psi(x)$  and  $\phi(t)$  obtained by solving the two ODE's are multiplied back together to find the final solution  $\Psi(x,t)$ . However, often our general solutions are in fact a superposition of many eigenstates. The contribution from each eigenstate depends on the initial state [1]. To explain how we do this, we must first explain how to use linear algebra to project a matrix from one basis onto another.

If we have two vectors,  $\mathbf{u}$  and  $\mathbf{v}$ , we can project  $\mathbf{u}$  onto  $\mathbf{v}$  by taking their dot product  $\mathbf{u} \cdot \mathbf{v} = \mathbf{v}^\dagger \mathbf{u}$ , which will give the scalar projection. We can then take that value and make it into a vector projection by multiplying in it by a unit vector in the same direction as  $\mathbf{v}$ . In symbolic terms, the scalar projection of  $\mathbf{u}$  onto  $\mathbf{v}$  is given by  $(\mathbf{v}^\dagger \mathbf{u}) * \mathbf{v} / v$ . If instead of one vector  $\mathbf{v}$  we had a set  $V$  of orthonormal vectors  $\mathbf{v}_1, \mathbf{v}_2, \dots, \mathbf{v}_n$ , we could project  $\mathbf{u}$  onto the set of vectors. For an orthonormal set,  $v=1$ , so the projection of  $\mathbf{u}$  onto  $V$  is given by  $(\mathbf{v}_1^\dagger \mathbf{u}) * \mathbf{v}_1 + (\mathbf{v}_2^\dagger \mathbf{u}) * \mathbf{v}_2 + \dots + (\mathbf{v}_n^\dagger \mathbf{u}) * \mathbf{v}_n$ . Each dot product gives a scalar coefficient, so we can define the coefficients as  $c_k = \mathbf{v}_k^\dagger \mathbf{u}$ . We can then write  $\mathbf{u} = c_1 * \mathbf{v}_1 + c_2 * \mathbf{v}_2 + \dots + c_n * \mathbf{v}_n$ .

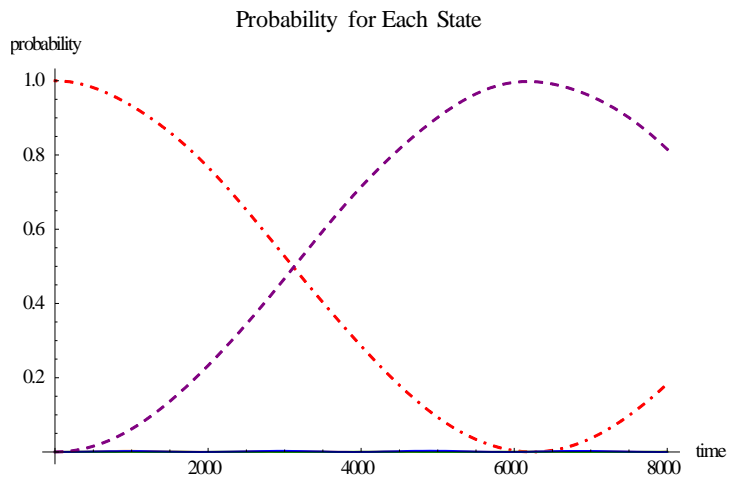
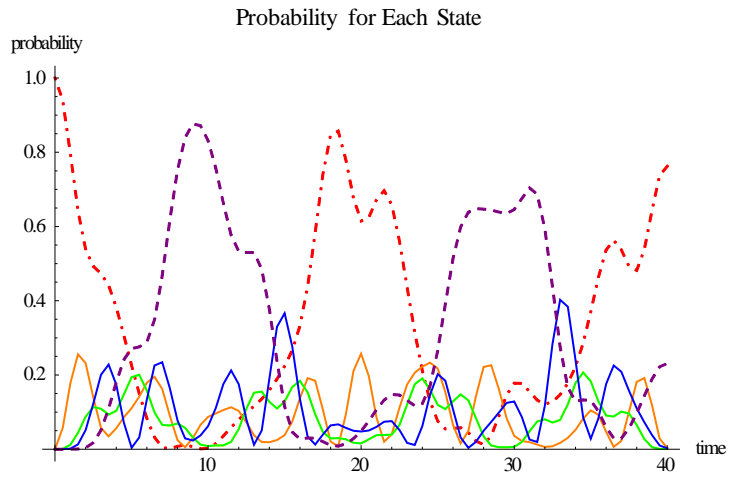
Now that we have explained projections, we can apply the concept to our system to help explain its dynamics. The  $\mathbf{u}$  from our example represents the initial state  $\Psi(0)$  and  $\mathbf{v}_k$  represents the  $k^{\text{th}}$  eigenvector of the Hamiltonian, or  $\psi_k$ . We choose as initial state a single site-basis vector. To find the dynamics of our system, we first project our initial state onto the basis of the eigenvectors. We then multiply each coefficient  $c_k = \mathbf{v}_k^\dagger \Psi(0)$  by the term  $e^{(-i * E_k * t)}$ , where  $E_k$  is the  $k^{\text{th}}$  eigenvalue. After we do this, we have  $\Psi(t)$  as a sum of the  $\psi_k$ 's and their coefficients. We can then collapse the vector back into the site basis by multiplying all of the coefficients by the vectors and adding the vectors. This will give  $\Psi(t)$  in the site basis with each coefficient time dependent.  $\Psi(t)$  is a linear combination of the different site

basis states. When the system is measured and we try to find out the orientation of each spin, only one basis vector is observed. The absolute value squared of each coefficient gives the probability of  $\Psi(t)$  being found in the corresponding basis vectors [18]:

$$P_l(t) = \left| \sum_{k=1}^D a_m^{(k)} a_l^{(k)} e^{-iE_k t} \right|^2. \quad (14)$$

When we plot all of the probabilities for all basis vectors together, we find interesting results, which depend on the value of  $\Delta$ , the boundary conditions, and the initial state. Examples are provided in Fig. 4. In the top panel of this figure, we consider an open chain and initial state  $|1100\rangle$ . This basis vector has energy  $+J\Delta/4$ . Its evolution is indicated by the dot-dashed line in the plot. For small  $\Delta$ , as time moves on the states with the highest probabilities of being observed are the ones with the same energy of the initial state, that is, the state  $|0011\rangle$  (dashed line). However, intermediate states with energies below  $J\Delta/4$  ( $-J\Delta/4$  or  $-3J\Delta/4$ ) will also appear in the process of getting from  $|1100\rangle$  to  $|0011\rangle$ , but with much lower probabilities than those of the states with the correct energy. As  $\Delta$  is increased, it takes much longer to get from  $|1100\rangle$  to  $|0011\rangle$ , with the time difference several magnitudes larger (middle panel of Fig. 4). This is because the flip flop term is no longer large enough to overcome the energy differences between the initial state and all the other intermediate states that result from the Ising interaction. It is as if the gaps in the histograms in the previous section become chasms where it is impossible to cross from one energy value to another. Also, the intermediate states will no longer appear on the graphs, as there will be zero probability of them being observed. This disappearance is because those states are now only virtual states and not real ones. When the system is closed instead of open and  $\Delta$  is kept large (bottom panel of Fig. 4), the time it takes to get from  $|1100\rangle$  to  $|0011\rangle$  is lessened, because there is now a choice of two directions to go to get from one state to another. Therefore, the

coupling between them happens in a lower order of perturbation theory [18]. Notice also that  $|0011\rangle$  is not the only state in resonance with  $|1100\rangle$  anymore. Since there are no more border effects,  $|0110\rangle$  and  $|1001\rangle$  have the same energy as the initial state and can also participate on its evolution.



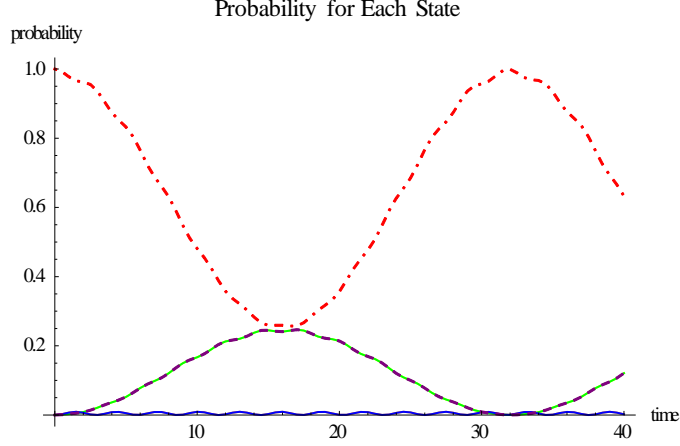


**Figure 4:** Probability of finding a state vs. time for the spin  $\frac{1}{2}$  system with nearest neighbor couplings;  $L=4$ ,  $N=2$ ,  $\Psi(0)=|1100\rangle$ . The dot-dashed line represents  $|1100\rangle$ , the dashed line represents  $|0011\rangle$ , and the other lines represent intermediate states. Top:  $\Delta=1$ , open boundary conditions. Middle:  $\Delta=10$ , open boundary conditions. Bottom:  $\Delta=10$ , closed boundary conditions. The visible solid line under the dashed line represent the states  $|1001\rangle$  and  $|0110\rangle$ .

We can also examine the magnetization of each site in time [18]. The magnetization is found using the following equation:

$$M_n(t) = \langle \Psi(t) | \hat{S}_n^z | \Psi(t) \rangle. \quad (15)$$

There is a maximum magnetization of  $+1/2$  which corresponds to an up spin, and a minimum magnetization of  $-1/2$  which corresponds to a down spin. It is possible to find a magnetization value between  $-1/2$  and  $+1/2$ , which corresponds to a superposition of up and down. From the graph of the magnetization, it is possible to see the excitations moving across the chain. For example, if our initial state has only one up spin on the beginning of the chain, as in the left panel of Fig. 5, the magnetization graph will show the up spin moving from one site to the next until it reaches the end of the chain. However, it is only the first and last site which will have the maximum magnetization; the other sites will only have some intermediate magnetization. This is because of border effects; the energy when the up spin is on the first and last sites is larger than when the up spin is on the intermediate sites. When  $\Delta$  becomes large, as in the right panel of Fig. 5, we no longer see the excitation moving along

the chain, because the intermediate states will be only virtual ones. Instead, on a much larger time scale, we will see the spin jumping from the first to the last site.

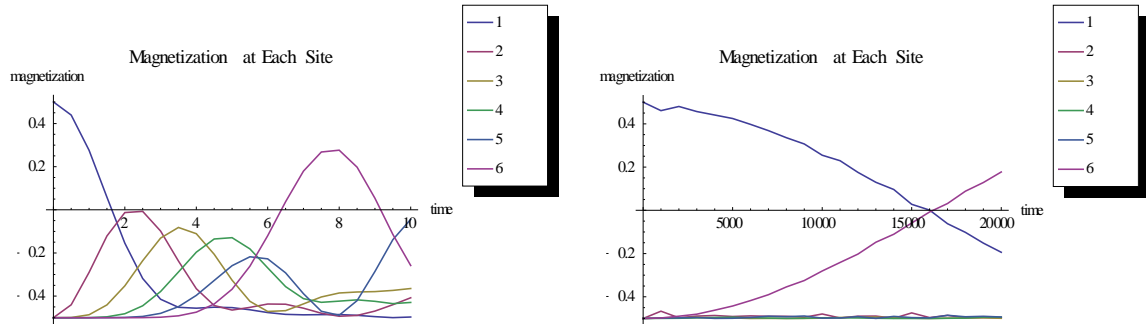


**Figure 5:** Magnetization of each site for the spin  $\frac{1}{2}$  system with nearest neighbor couplings and open boundary conditions;  $L=6$ ,  $N=1$ ,  $\Psi(0)=|100000\rangle$ . Left:  $\Delta=0.5$ . Right:  $\Delta=10$ .

## IV.7. Symmetries

The symmetries of the system can also be helpful in explaining its dynamics. First we will explain what those symmetries are, and then we will explain how to make use of those symmetries to predict the dynamics of the system.

We have already stated that total spin in the  $z$ -direction,  $S^z = \sum_j S_j^z$  is conserved [ $H, S^z] = 0$ . There are other conserved quantities in our system as well, which can be represented by operators and arise from symmetries in the system. Therefore, in the dynamics of the system, the conserved quantities will remain constant, which will limit the eigenstates which will participate in the dynamics.

One type of symmetry is reflection, which leads to conservation of parity. Parity occurs when we have a state which is a mirror image of itself. An example of a state with reflectional symmetry is  $|110000\rangle + |000011\rangle$ . Depending on the sign in the middle, we call parity even or odd; a  $+$  corresponds to even parity, while a  $-$  corresponds to odd parity. If  $P$  is the parity operator, its effect is

$$P[|110000\rangle + |000011\rangle] = (+1) [|000011\rangle + |110000\rangle].$$

$$P[|110000\rangle - |000011\rangle] = [|000011\rangle - |110000\rangle] = (-1) [|110000\rangle - |000011\rangle]. \quad (16)$$

Another symmetry we need to take into account is related to a  $\pi$ -rotation of the spins of the system around a direction perpendicular to  $z$ . This rotation corresponds to flipping each of the spins in the first state in the combination to get the second state. An example of a state with rotational symmetry is  $|110000\rangle + |001111\rangle$ . Again, the sign in between the two states is important; if the sign is  $+$ , we say that the eigenvalue of the operator realizing the rotation is equal to  $+1$ , and if the sign is  $-$ , we say the eigenvalue of the operator realizing the rotation is equal to  $-1$ . In our system, since  $S^z$  is conserved, invariance over a global  $\pi$ -rotation occurs only when the number of up-spins is  $N=L/2$  ( $L$  is even). If  $R_x^\pi$  is the  $\pi$ -rotation operator, its effect is:

$$R_x^\pi [|1001\rangle + |0110\rangle] = +1 [|0110\rangle + |1001\rangle]$$

$$R_x^\pi [|1001\rangle - |0110\rangle] = [|0110\rangle - |1001\rangle] = (-1) [|1001\rangle - |0110\rangle]. \quad (17)$$

There are some states, such as  $|111000\rangle + |000111\rangle$ , which exhibit both symmetries, parity and rotation. The system may exhibit other symmetries that we will not discuss here, such as total spin on an isotropic chain or translation on a closed chain [18].

In our clean system with open boundary conditions and  $N=L/2$ , each eigenvector is an eigenstate of the parity operator and of the  $\pi$ -rotation operator. If we project our initial state containing one type of parity onto the eigenvector basis, the only eigenvectors which will contribute will be the ones with the same type of parity. For example, if our initial state has even parity, all contributing eigenstates contributing to the evolution of the state will have even parity. Since we have no information about the  $\pi$ -rotation, eigenvectors with either type of  $\pi$ -rotation can contribute. Similarly, if we project our initial state containing one type of  $\pi$ -

rotation symmetry onto the eigenvector basis, the only eigenvectors which will contribute will be the ones with the same type of rotation eigenvalue for the  $\pi$ -rotation operator, but the parity will not matter. We can also project an initial state which has both parity and rotational symmetry, and the result will be that only eigenvectors which match both types of symmetry will participate in the evolution of the initial state. For this reason, the symmetries of the system restrict the system's dynamics, as can be seen when we plot the symmetries in time.

We can plot the dynamics of the system to see its symmetry in time in two ways. For both, we need to create the XX basis. This is the basis which corresponds to the eigenvectors of a matrix consisting of the non-diagonal elements of the Hamiltonian. The first way to plot the dynamics of the system is to plot the dynamics the same way we did earlier, but then to project our final  $\Psi(t)$  onto the XX basis before graphing. The second way is to multiply our regular Hamiltonian matrix by the XX basis in front and its inverse afterwards to get a new matrix. We use the same method as before to find  $\Psi(t)$ , except that we write our initial state in terms of the XX basis and use the eigenvectors of the new matrix instead of the original Hamiltonian matrix. Regardless of the method used, the graphs as seen in Fig. 6 show that in time, the system will continue to exhibit the same types of symmetries as it did in the initial state, which further proves that symmetry is conserved.

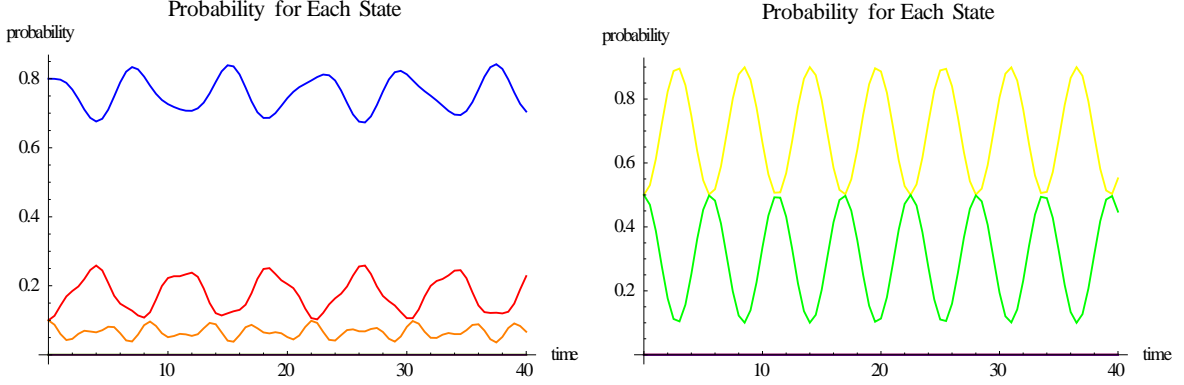


**Figure 6:** Dynamics of the the spin  $\frac{1}{2}$  system with nearest neighbor couplings and open boundary conditions;  $L=4$ ,  $N=2$ ,  $\Delta=0.5$ . Left: even parity,  $\Psi(0)=(|1100\rangle+|0011\rangle)/\sqrt{2}$ . Right: odd parity,  $\Psi(0)=(|1100\rangle-|0011\rangle)/\sqrt{2}$ .

Now that we have explained the spin-1/2 chain with nearest neighboring couplings in depth, we can now explain how to detect the quantum phase transitions in this system. Based on our studies of the spectrum above, we can predict that these transitions will relate to the presence or absence of the gaps in the spectrum.

### V.1. Detecting Phase Transitions

There have been different methods suggested for detecting quantum phase transitions. Most of these methods borrow tools from quantum information. The first major category of detecting quantum phase transitions is entanglement. This category includes several quantities. Concurrence is a measure of the pairwise entanglements of particles in the system. Entanglement entropy measures the entropy of a subsystem of the larger system. Quantum discord measures the quantumness of the system by finding the difference between the classical information and the concurrence [6].

Another quantity used to detect quantum phase transitions is the fidelity. The fidelity of a system is a measurement of how two states overlap when a parameter is varied slightly:

$$F = |\langle \Psi(g) | \Psi(g + \delta) \rangle|. \quad (18)$$

Generally, since the states are normalized and the change in the parameter is small, the fidelity will be close to one. However, at a transition, the overlap is small even if the parameter changes very little. This is because at the transition, the states become orthogonal to each other since they are in different phases [6].

A possible problem with this method is what is known as the orthogonality catastrophe. To use the fidelity of the system, states should not be orthogonal to each other except at a critical point. However, at the thermodynamic limit, even when there is no critical point the states are still orthogonal to each other. Nevertheless, in finite systems the states become orthogonal more quickly near critical points due to the large amount of degrees of freedom, so we are still able to take advantage of the orthogonality to detect the transitions [19].

Another quantity, the one which is the focus of this research, is the invariant correlational entropy of the system, or the ICE. Unlike the fidelity, this method is not basis-specific. This entropy also measures how responsive a system is when one of its parameters is changed [12]. To compute the invariant correlation entropy, a density matrix  $\rho$  is calculated from the ground state or first excited state eigenvectors of the Hamiltonian matrix:

$$\rho = |\Psi\rangle\langle\Psi|. \quad (19)$$

Several density matrices with different values of the parameter considered over a small range are then averaged together:

$$\bar{\rho} = \frac{\rho_g + \rho_{g+\delta} + \dots + \rho_{g+(N-1)\delta}}{N}. \quad (20)$$

The ICE entropy  $S$  corresponds to von Neumann entropy calculated from this averaged density matrix of the system,  $\bar{\rho}$ , using the following equation [12]:

$$S = -\text{Tr} \{ \bar{\rho} \ln(\bar{\rho}) \}. \quad (21)$$

Calculating an averaged density matrix is necessary, because otherwise the system would be pure and its Von Neumann entropy would be zero, which is trivial. By averaging the density matrices, the system becomes a mixed system, and the entropy has a non-trivial value.

The entropy is calculated for many different averaged density matrixes centered around different values of the parameter. When the entropy is graphed vs. the varied parameter, the graph should exhibit a peak where there is a phase transition. This is because at a phase transition, the system is more sensitive to the parameter change.

## **V.2. Results of Using ICE to Detect Phase Transitions**

We will show results for the ICE for two models of spin-1/2 systems with periodic boundary conditions. One is the Heisenberg model with nearest neighbor (NN) couplings, explained in depth earlier (Equation (4)); the other is a Heisenberg model that also takes into account couplings between next nearest neighbors (NNN).

Studies of quantum phase transition usually focus on the ground state. In our spin systems, however, the transition is captured by studying the first excited state, and not the ground state.

For the Heisenberg model, the two terms in competition are the Ising interaction and the flip flop term (see Equation (4)). When  $\Delta$  is less than -1, the system is in the ferromagnetic phase, with all spins of the ground state pointing in the same direction. At  $\Delta = -1$ , there is a first order phase transition [7]. Since this transition is easy to detect, we did not focus on it. When  $\Delta$  is between -1 and 1, the system is the xy phase, or the gapless phase [9]. In this phase, the energy bands are indistinct, and spins can move easily throughout the chain,

typical of a conductor. A BKT-type critical point occurs when the strength of the Ising interaction is equal to the strength of the flip flop term, or  $\Delta=1$  [7]. This transition is hard to detect, and is therefore the focus of this research. When  $\Delta>1$ , the system becomes antiferromagnetic, with spins of the ground state pointing in alternating directions. The system becomes an insulator because the gaps the energy bands result in a long time frame for the motion of spins.

The energy for this system, as shown in Fig. 7, is also telling. When  $\Delta<-1$ , the ground state is degenerate, as is the first excited state. At  $\Delta=-1$ , the ground state breaks up into a new ground state which is a singlet with total spin in the z direction  $S^z=0$ , and a degenerate first excited state with  $S^z=-1$  and 1. At  $\Delta=1$ , the ground state remains unchanged, but the first excited state breaks up again. The new first excited state has  $S^z=0$ .

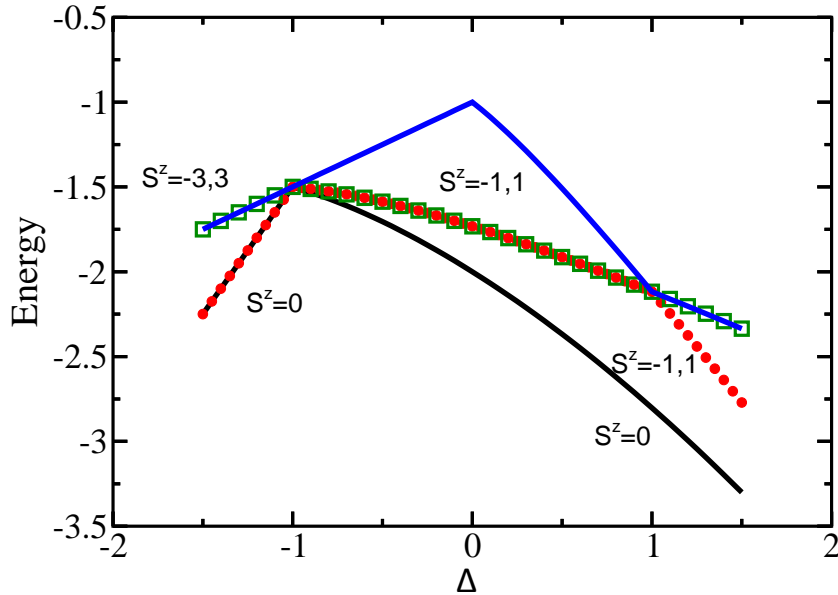


**Figure 7:** Energy of the Heisenberg model with NN couplings and closed boundary conditions as  $\Delta$  is varied. We show the ground state and the first excited state, as well as the states these break up into when the states start out degenerate.

The fidelity of the graph is as expected. Our graph includes only  $\Delta>0$ , because we were only examining the second critical point. We graphed the fidelity for the first excited

state, since the ground state did not give any results in this region of values for  $\Delta$  which we were considering. Our results are shown in Fig. 8. We found that the fidelity was equal to 1, signifying almost complete overlap between the states, except at the critical point  $\Delta=1$ , where the fidelity dropped to zero. When examining the energy graph, this makes sense. Before  $\Delta=1$ ,  $S^z$  for the first excited state was -1 or 1, while after  $\Delta=1$ ,  $S^z$  was 0. Since the spins are different, the states must therefore be orthogonal, and so the fidelity drops.

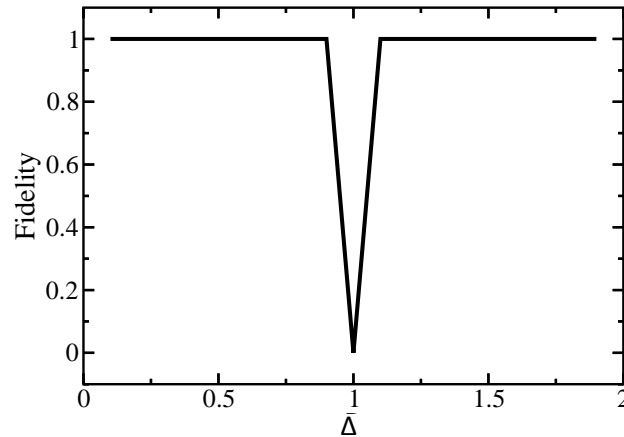


**Figure 8:** Fidelity vs.  $\Delta$  for the Heisenberg model with NN couplings and closed boundary conditions for  $L=10$ .

We also examined the ICE for the system. The results for the first excited state, as shown in Fig. 9, reflected the results from the fidelity. The ICE was zero, except for at the critical point when it peaked.

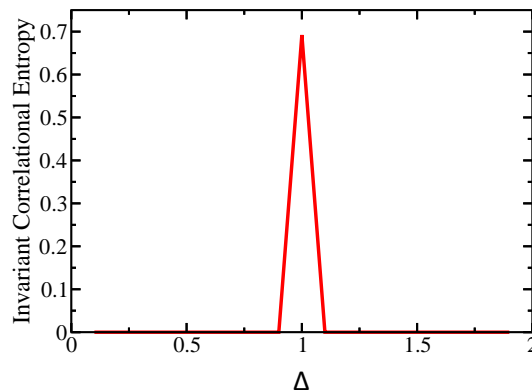


**Figure 9:** ICE vs.  $\Delta$  for the Heisenberg model with NN couplings and closed boundary conditions for  $L=10$

The similarity to the fidelity graph makes sense, because the fidelity is similar to the ICE for if only two states were averaged. An advantage of the ICE over the fidelity, however, is that it is sensitive enough to detect critical points while using the ground state, which the fidelity cannot do while the system is small. We graphed the ICE for different sizes of the system in the ground state. Our results are shown in Fig. 10. For each of the curves on the entropy graph, there is an inflection point at the critical point, which is signified by the dotted line.

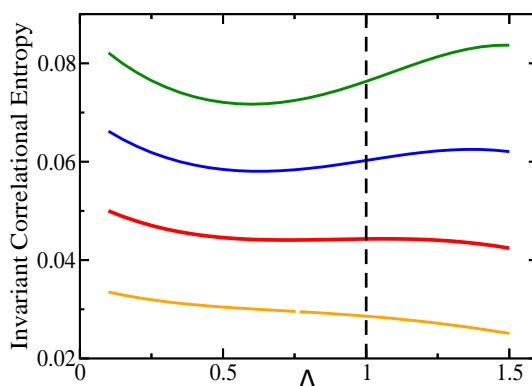


**Figure 10:** ICE of the Heisenberg model with NN couplings and closed boundary conditions vs.  $\Delta$ . From bottom to top, the size of the system is  $L=6$ ,  $L=8$ ,  $L=10$ ,  $L=12$ .

The second system has both NN and NNN couplings. The ratio between the strength of this additional interaction and the NN couplings is characterized by the parameter  $\lambda$ . The equation for the system is given as follows:

$$H = \sum_{j=1}^L S_j S_{j+1} + \lambda S_j S_{j+2} . \quad (22)$$

The quantum phase transition is driven by the competition between the NN and NNN interaction [20]. The critical point occurs close to  $\lambda=0.2411$ . This critical point has not yet been found analytically, but rather has been found from numeric studies based on where an energy gap appears. Before the critical point, the system is in a fluid phase; after, it is in the

dimer phase. There is another critical point at  $\lambda=0.5$ , called the Majumdar-Ghosh point, but since this is not a BKT-type transition it is easier to detect [20].

Again, we graphed the energies of the system. Our results are shown in Fig. 11. When  $\lambda$  was less than 0.241, the ground state was a singlet with  $S^z=0$ , and the first excited state was a triplet with  $S^z=-1, 0$ , and 1. After  $\lambda =0.241$ , the first excited state split, and the new first excited state was a singlet with  $S^z=0$ . Because there is a state with  $S^z=0$  before and after the critical point, we were able to examine the quantum phase transition using only this subspace.

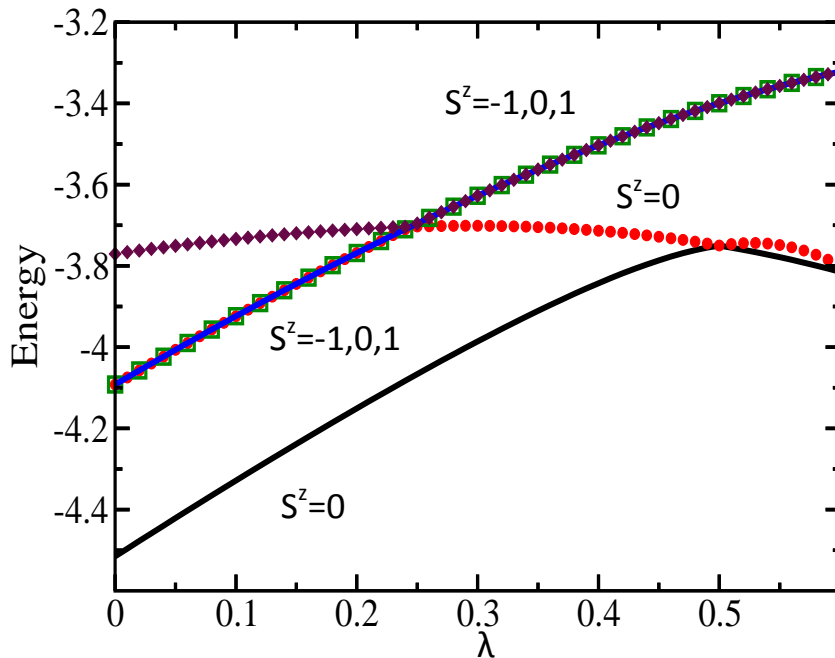


**Figure 11:** Energy of the NNN model with closed boundary conditions as  $\lambda$  is varied. We show the ground state and the first excited state, as well as the states that become degenerate with these states.

While the ICE is able to detect the Majumdar-Ghosh point in the ground state, neither it nor the fidelity was able to detect the BKT-type critical point for the ground state. Instead, we used the first excited state for all graphs. In Chen et. al's paper, they graphed the fidelity of the system vs. the parameter for several different sizes of the system [20] (See left panel of Fig. 12). For each, the fidelity was one except by the critical point, where it was zero. The

drop did not occur exactly at 0.2411 for each system; however, as the system got larger, the measured critical point got closer to that value. Again, our results for the ICE reflected the results for the fidelity, as seen in the right panel of Fig. 12. Also, like the fidelity, as our system got larger the detected critical point became closer to the accepted value.

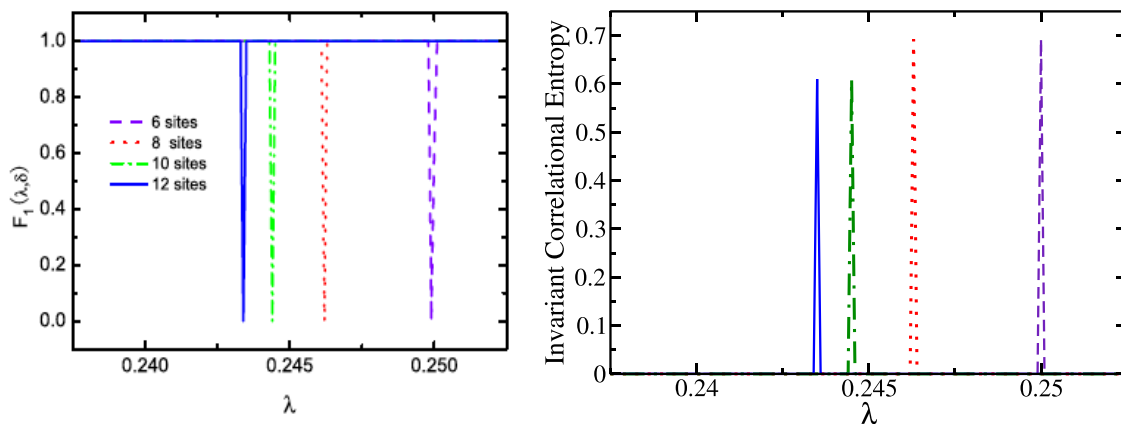


**Figure 12:** Left: Chen et. al.'s [20] plot of fidelity vs.  $\lambda$  for the NNN model, for different values of  $L$ . Right: ICE vs.  $\lambda$  for the NNN model for different values of  $L$ . From right to left, the peaks are for system sizes  $L=6$ ,  $L=8$ ,  $L=10$ ,  $L=12$ .

## VI. Conclusions

We have seen that the invariant correlational entropy is a good tool to detect quantum phase transitions. This method has some benefits over similar quantities such as the fidelity. This is because it is sensitive to transitions in the ground state, and is basis independent. However, it is unclear to what extent this method will be more useful than the other methods that exist now, rather than just repeating the results of those methods.

There are two main directions for our future research. One direction is to study the ICE for more systems. For example, we would like to study the ICE in more detail for the Ising model with a transverse field, and for Bose-Einstein condensates. The other main direction is to use *Fortran* to study larger systems. When we do this, we will be able to

conduct a scaling analysis to extrapolate what the calculated value of the critical point would be for an infinite size system, to see if it would match the accepted value. Chen et. al. already conducted such an analysis for the next nearest neighbor system using the fidelity [20]. We would like to reproduce his results using the ICE, and would also like to complete this analysis for the other systems.

### **Acknowledgements**

I would like to thank Dr. Lea F. Santos for assisting me on my project and for her willingness to work with me and explain things when necessary. I would like to thank Dr. Wachtell and the S. Daniel Abraham Honors Program for encouraging me to conduct research and giving me other enriching opportunities throughout my undergraduate experience. I would like to thank Dr. Kressel for the funding to perform research this year and to present my work at the American Physical Society March Meeting, and the Kressel Committee and Deans for awarding me the Kressel Fellowship. I would like to thank Kira Joel for her collaboration for some parts of this research.

### **References**

- [1] D. J. Griffiths, *Introduction to Quantum Mechanics* (Prentice Hall, Second edition.)
- [2] S. Sachdev, "Quantum phase transitions," *The New Physics*, G. Fraser, Ed.  
[http://qpt.physics.harvard.edu/newphysics\\_sachdev.pdf](http://qpt.physics.harvard.edu/newphysics_sachdev.pdf).
- [3] S. Sachdev, *Quantum Phase Transitions* (Cambridge University Press, ed. 2)
- [4] M. Greiner, S. Frolig, Optical lattices. *Nature* **453**, p. 736-738 (2008).

- [5] G. G. Batrouni and R. T. Scalettar, *Quantum Phase Transition*, in "Ultracold Gases and Quantum Information", Lecture Notes of the Les Houches Summer School in Singapore, **91** (Oxford University Press, 2009).
- [6] A. Dutta, U. Divakaran, D. Sen, B. K. Chakrabarti, T. F. Rosenbaum, G. Aeppli, "Quantum phase transitions in transverse field spin models: from statistical physics to quantum information," arXiv 1012.0653v2 (25 Nov 2012).
- [7] L. Justino, T. R. de Oliveira, "Bell inequalities and entanglement at quantum phase transitions in the XXZ model," *Physical Review A* **85**, 052128 (2012).
- [8] R. K. Pathria, *Statistical Mechanics* (Elsevier, Oxford, 2005).
- [9] H.-J Mikeska and A. K. Kolezhuk, *One-Dimensional Magnetism*, in Lecture Notes in Physics **645** (Springer, Berlin 2004).
- [10] L. F. Santos, A. Polkovnikov, M. Rigol, "Entropy of isolated quantum systems after a quench," *Physical Review Letters* **107**, p.040601 (2011).
- [11] A. Ben-Naim. *Entropy Demystified* (World Scientific, New Jersey, Revised ed., 2008).
- [12] A. Volya, V. Zelevinsky, "Invariant correlational entropy as a signature of quantum phase transitions in nuclei," *Physics Letters B* **574**, p. 27-34 (2003).
- [13] M. Greiner, O. Mandel, T. Esslinger, T. Hänsch, I. Bloch, "Quantum phase transition from a superfluid to a Mott insulator in a gas of ultracold atoms," *Nature* **415**, p. 39-44 (2002).
- [14] R. Feynman, *Six Easy Pieces: essentials of physics explained by its most brilliant teacher* (Helix Books, Reading, Mass., 1995).
- [15] J. C. Kotz, P. M. Treichel, and G. C. Weaver. *Chemistry & chemical reactivity* (Thompson Brooks/Cole, Belmont, CA, 6<sup>th</sup> edition, 2006).

- [16] R. Eisberg, R. Resnick, *Quantum physics of atoms, molecules, solids, nuclei, and particles* (Wiley, New York, 1985), Chapt 8&14.
- [17] C. R. Nave, “Quantum Physics,” *Hyperphysics*, Georgia State University, <http://hyperphysics.phy-astr.gsu.edu/hbase/hframe.html> (2012).
- [18] K. Joel, D. Kollmar, L. F. Santos, “An introduction to the spectrum, symmetries, and dynamics of Heisenberg spins-1/2 chains,” arXiv 1209.0115 (1 Sep 2012).
- [19] P. Zanardi, N Paunkovic, “Ground state overlap and quantum phase transitions,” *Physical Review E* **74**, 031123 (2006).
- [20] S. Chen, L. Wang, S. Gu, Y. Wang, “Fidelity and Quantum phase transition for the Heisenberg chain with the next-nearest-neighbor interaction,” *Physical Review E* **76**, 061108 (2007).